DOI: 10.13009/EUCASS2025-437
11TH EUROPEAN CONFERENCE FOR AERONAUTICS AND SPACE SCIENCES (EUCASS)

A New Analytical Solution for Swirl Propagation in Rocket Nozzles and its Application for Combustion Efficiency Evaluation

Valerio Santolini[⋆], *Federico Giambelli*[⋆], *Alessio Nisticó*[⋆] *and Christian Paravan*[⋆†]
[⋆]*Space Propulsion Laboratory, Aerospace Science and Technology Department, Politecnico di Milano*
Via La Masa 34, Milano, Italy, I-20156
valerio.santolini@polimi.it · federico.giambelli@polimi.it · alessio.nistico@polimi.it · christian.paravan@polimi.it
[†]Corresponding author

Abstract

Swirl injection is a widely used strategy to improve performance in liquid and hybrid rocket engines. However, the gas flow can sometimes retain part of the tangential velocity component when entering the engine nozzle. This can lead to an apparent contraction of the throat diameter with respect to its geometrical value [1, 2]. Ignoring this effect can lead to undesired biases as, for example, an overestimation of the combustion efficiency when the latter, expressed as the characteristic velocity ratio, makes use of the classical equation function of the throat section to compute the experimental characteristic velocity [2, 3].
This work develops a quasi-1-dimensional mathematical model describing the gas-dynamic expansion of hot gases in a nozzle for flows with axial and tangential velocity. The proposed model becomes the Shapiro equations [4] when the tangential component is null.
The mathematical solution has been used to develop a numerical model for the swirl correction of the experimental data related to the Vortex Flow Pancake, a hybrid rocket engine in use at the Politecnico di Milano Space Propulsion Laboratory (SPLab) and characterized by a full tangential injection of the oxidizer [5, 6].

1. Introduction

Swirling injection is a widely implemented strategy to improve the performance of hybrid rocket engines (HRE) [5, 7, 8]. Traditional hybrid rockets suffer from slow solid-fuel regression rates, low volumetric loading, and relatively poor combustion efficiency. Swirl injection enhances performance by introducing a strong tangential velocity component to the oxidizer in the combustion chamber, resulting in increased regression rates and combustion efficiency [3, 9–15]. The tangential velocity component tends to diminish as the flow moves toward the exit, as rocket nozzles are designed to accelerate gas in the axial direction. However, if the combustion chamber and post-chamber lengths are insufficient and the initial flow is highly swirled, the gas may retain its swirl as it expands through the nozzle [2, 16–18]. Consequently, evaluating combustion chamber efficiency using traditional methods can lead to overestimation, with values that could exceed 100% [1, 5, 19, 20]. Different alternative approaches have been proposed for calculating the efficiency of the combustion chamber in the presence of swirling flows [6, 19, 20]. Yuasa et al. [19] proposed a technique to indirectly evaluate the characteristic velocity c^* efficiency using the specific impulse efficiency and thrust coefficient. Santolini et al. [6] proposed a numerical-experimental approach that uses the thrust measurement to compute the throat-contraction and use it to correct the c^*.

This paper develops an analytical solution to swirling flows through a nozzle as a quasi-1D flow. The developed equations are found to be extensions of Shapiro's equations and they coincide when the tangential velocity is null. Application of the quasi-1D model shows the effect of throat-contraction with respect to non-swirling flows, that allows to correct the combustion efficiency.

DOI: 10.13009/EUCASS2025-437

2. Analytical Model

2.1 Starting Equations

Conservation Equations

Let's write the conservation of mass, momentum and energy for 3-dimensional inviscid fluid, negligible gravity contribution, no external work but allowing a possible heat flux:

$$\frac{\partial \rho}{\partial t} + \vec{u} \cdot (\nabla \rho) + \rho(\nabla \cdot \vec{u}) = 0 \tag{1}$$

$$\frac{\partial \vec{u}}{\partial t} + (\vec{u} \cdot \nabla)\vec{u} + \frac{\nabla p}{\rho} = \vec{0} \tag{2}$$

$$\frac{\partial(\rho h)}{\partial t} - \frac{\partial p}{\partial t} + \nabla \cdot (\rho \vec{u} h) + \frac{\partial(\rho k)}{\partial t} + \nabla \cdot (\rho \vec{u} k) = \nabla \cdot \vec{Q} \tag{3}$$

where the defined variables are: t - time, ρ - density, $\vec{u}$ - velocity vector, p - pressure, h - specific enthalpy, k - specific kinetic energy, and $\vec{Q}$ - heat flux. The operator ∇ is the gradient while $(\nabla \cdot)$ is the divergence.

Other Useful Equations and Identities

Apart from the previously defined main equations, it is also useful to define the following.

The law of **perfect gas**:

$$p = \frac{\rho R_u T}{\mathcal{M}} = \rho R T \tag{4}$$

where: T - temperature, R_u - universal gas constant, $\mathcal{M}$ - molar mass, and R - specific gas constant. The gradient of Eq. (4) leads to the two equivalent equations that follows:

$$\frac{\nabla p}{p} = \frac{\nabla \rho}{\rho} + \frac{\nabla T}{T} - \frac{\nabla \mathcal{M}}{\mathcal{M}} \qquad or \qquad \frac{\nabla p}{p} = \frac{\nabla \rho}{\rho} + \frac{\nabla T}{T} + \frac{\nabla R}{R} \tag{5}$$

The **sonic velocity**:

$$a^2 = \gamma R T \tag{6}$$

where: a - sonic velocity, and γ - specific heat ratio. The gradient of Eq. (6) follows as the two equivalent equations:

$$\frac{\nabla a}{a} = \frac{1}{2}\left(\frac{\nabla \gamma}{\gamma} + \frac{\nabla T}{T} - \frac{\nabla \mathcal{M}}{\mathcal{M}}\right) \qquad or \qquad \frac{\nabla a}{a} = \frac{1}{2}\left(\frac{\nabla \gamma}{\gamma} + \frac{\nabla T}{T} + \frac{\nabla R}{R}\right) \tag{7}$$

The **Mach number**:

$$\vec{\mathrm{Ma}} = \vec{u}/a \qquad \mathrm{Ma}^2 = u^2/a^2 \qquad Ma_i^2 = u_i^2/a^2 \tag{8}$$

where $\vec{\mathrm{Ma}}$ - the mach number vector, Ma - the magnitude of the Mach vector, u - the magnitude of the velocity vector, and the subscript $_i$ indicates a single component of the vector. Let's compute the gradient of Mach number of Eq. (8):

$$\nabla \mathrm{Ma}^2 = \nabla\left(\frac{u^2}{a^2}\right) = \frac{\nabla u^2}{a^2} - \frac{u^2}{a^4}\nabla a^2 \tag{9}$$

that can be written as follow by multiplying everything for a^2/u^2:

$$\frac{\nabla \mathrm{Ma}^2}{\mathrm{Ma}^2} = \frac{\nabla u^2}{u^2} - \frac{\nabla a^2}{a^2} \tag{10}$$

by substituting Eq. (7) it follows:

$$\frac{\nabla \mathrm{Ma}^2}{\mathrm{Ma}^2} = \frac{\nabla u^2}{u^2} - \frac{\nabla \gamma}{\gamma} - \frac{\nabla T}{T} - \frac{\nabla R}{R} \tag{11}$$

Thanks to the identity of Eq. (8), this is true for every component as well.

DOI: 10.13009/EUCASS2025-437

The **specific heat capacity**:

$$c_p = \frac{\gamma}{\gamma - 1} R \tag{12}$$

where c_p is the specific heat capacity. Coupling Eq. (12) and (6) leads to the following identity:

$$c_p T = \frac{a^2}{\gamma - 1} \tag{13}$$

The **entropy**:

$$T\nabla s = c_p \nabla T - \frac{\nabla p}{\rho} \qquad or \qquad \frac{\nabla s}{c_p} = \frac{\nabla T}{T} - \frac{\gamma - 1}{\gamma} \frac{\nabla p}{p} \tag{14}$$

where s is the entropy.

2.2 General Quasi-1D Differential Equations: derivation

Let's add the simplification of steady-state (st.s.) flow. It is convenient to consider the problem in cylindrical coordinates: z - axial coordinate, θ - tangential coordinate, and r - radial coordinate. The flow is considered axisymmetric, thus the partial derivatives in the tangential direction are null: $\partial()/\partial\theta = 0$. Furthermore, for an axisymmetric flow with a sufficiently gradual change in the cross section of the nozzle, the radial velocity and its derivatives are often considered negligible in the literature [2, 21–25]. The same is assumed in this work.

After these hypotheses, the previous equations may be rewritten as follow.

From the mass equation

The mass equation of Eq. (1) simplifies due to the st.s. condition:

$$\nabla \cdot (\rho \vec{u}) = 0 \tag{15}$$

The Eq. (15) can be integrated on a control volume of radius r. By using the divergence theorem, it leads to the following equation:

$$d(\rho u_z r^2) = 0 \tag{16}$$

where d denotes the partial derivative in the axial direction $\partial()/\partial z$, r^2 is – simplified of the π term – the nozzle cross-sectional area up to the reference radius r, and that ρ and u_z are assumed to be uniform in the radial direction. Another way to express Eq. (16) is as follows:

$$\frac{d\rho}{\rho} + \frac{du_z}{u_z} + \frac{dr^2}{r^2} = 0 \tag{17}$$

From the momentum equation

The momentum equation of Eq. (2) simplifies due to the st.s. condition:

$$(\vec{u} \cdot \nabla)\vec{u} + \frac{\nabla p}{\rho} = 0 \tag{18}$$

The vector equation becomes three scalar equations when expressed in the reference frame of choice. In cylindrical coordinates, the following equation is the momentum axial component:

$$\cancel{u_r} \frac{\partial u_z}{\partial r} + \frac{u_\theta}{r} \cancel{\frac{\partial u_z}{\partial \theta}} + u_z \frac{\partial u_z}{\partial z} + \frac{1}{\rho} \frac{\partial p}{\partial z} = 0 \tag{19}$$

where some terms cancel out due to the hypotheses made. By doing some arithmetic and making use of Eq. (4), (6) and (8):

$$u_z du_z + \frac{dp}{\rho} = 0 \tag{20}$$

DOI: 10.13009/EUCASS2025-437

$$\frac{1}{2}du_z^2 + \frac{dp}{\rho} = 0$$
$$\frac{1}{2}\frac{\rho}{p}du_z^2 + \frac{dp}{p} = 0$$
$$\frac{1}{2}\frac{1}{RT}du_z^2 + \frac{dp}{p} = 0$$
$$\frac{1}{2}\frac{\gamma}{a^2}du_z^2 + \frac{dp}{p} = 0$$
$$\frac{1}{2}\gamma\frac{u_z^2}{a^2}\frac{du_z^2}{u_z^2} + \frac{dp}{p} = 0$$
$$\frac{1}{2}\gamma \mathrm{Ma}_z^2\frac{du_z^2}{u_z^2} + \frac{dp}{p} = 0 \tag{21}$$

From the rotor of momentum equation (vorticity equation)

Let's now derive the vorticity equation by making the rotor ($\nabla\times$) of the momentum equation of Eq. (18):

$$\nabla \times ((\vec{u}\cdot\nabla)\vec{u}) + \nabla \times (\frac{\nabla p}{\rho}) = \vec{0} \tag{22}$$

It follows that, by making use of vector calculus identities:

$$(\vec{u}\cdot\nabla)\vec{w} = (\vec{w}\cdot\nabla)\vec{u} - \vec{w}(\nabla\cdot\vec{u}) + \frac{\nabla p \times \nabla\rho}{\rho^2} \tag{23}$$

where $\vec{w}$ is the vorticity and is defined as $\vec{w} \doteq \nabla \times \vec{u}$. It is of interest to explicit the axial component of the equation in cylindrical coordinates. Recall that due to the axial symmetry hypothesis, the derivatives $\partial(\,)/\partial\theta$ are null. This cancels out from the axial component many velocity-related terms and the density-pressure related term. Thus, the axial component of the equation becomes:

$$\cancel{u_r}\frac{\partial w_z}{\partial r} + u_z\frac{\partial w_z}{\partial z} = w_r\frac{\partial u_z}{\partial r} + w_z\frac{\partial u_z}{\partial z} - w_z\left(\frac{1}{r}\cancel{\frac{\partial(ru_r)}{\partial r}} + \frac{\partial u_z}{\partial z}\right) \tag{24}$$

where the canceled terms are because $u_r \sim 0$. Therefore, the axial component of the vorticity equation becomes:

$$u_z\frac{\partial w_z}{\partial z} = w_r\frac{\partial u_z}{\partial r} \tag{25}$$

or, by replacing the vorticity with the velocity:

$$u_z\frac{\partial}{\partial z}\left(\frac{1}{r}\frac{\partial(ru_\theta)}{\partial r}\right) + \frac{\partial u_\theta}{\partial z}\frac{\partial u_z}{\partial r} = 0 \tag{26}$$

The axial velocity u_z was assumed uniform in the radial direction in Eq. (16). This assumption leads to neglecting the second term of Eq. (26), which results in the conservation of vorticity axial component:

$$d\left(\frac{1}{r}\frac{\partial(ru_\theta)}{\partial r}\right) = 0 \tag{27}$$

or

$$dw_z = 0 \tag{28}$$

By integrating on an area of radius r – simplifying the π term – it follows:

$$d\left(\int_0^r \frac{1}{\tilde{r}}\frac{\partial(\tilde{r}u_\theta)}{\partial\tilde{r}}\tilde{r}\,d\tilde{r}\right) = 0$$
$$d\,(r\,u_\theta) = 0 \tag{29}$$

Another way to express Eq. (29) is as follows:

$$\frac{dr}{r} + \frac{du_\theta}{u_\theta} = 0 \qquad or \qquad \frac{1}{2}\frac{dr^2}{r^2} + \frac{du_\theta}{u_\theta} = 0 \qquad or \qquad \frac{dr^2}{r^2} + \frac{du_\theta^2}{u_\theta^2} = 0 \tag{30}$$

DOI: 10.13009/EUCASS2025-437

From the energy equation

The energy equation (3) simplifies due to the st.s. condition:

$$\nabla\cdot(\rho\vec{u}h) + \nabla\cdot(\rho\vec{u}k) = \nabla\cdot\vec{Q} \tag{31}$$

By defining $\vec{Q} \doteq \rho\vec{u}q$ – where q is the specific heat – it follows:

$$\nabla\cdot(\rho\vec{u}h) + \nabla\cdot(\rho\vec{u}k) = \nabla\cdot(\rho\vec{u}q) \tag{32}$$

By making use of Eq. (15) it becomes:

$$\rho\vec{u}\cdot\nabla(h + k - q) = 0 \tag{33}$$

The gradient of enthalpy can be expressed as $\nabla h \doteq c_p\nabla T$. By exploiting this definition and dividing everything by c_pT, it follows:

$$\rho\vec{u}\cdot\left(\frac{\nabla T}{T} + \frac{\nabla k}{c_pT} - \frac{\nabla q}{c_pT}\right) = 0 \tag{34}$$

Notice that the kinetic term can be expressed as follow by using Eq. (13) and (8):

$$\frac{\nabla k}{c_pT} = \frac{\nabla u^2}{2}\frac{\gamma-1}{a^2} = \frac{\gamma-1}{2}\mathrm{Ma}^2\frac{\nabla u^2}{u^2} \tag{35}$$

Thus, substituting Eq. (35) into Eq. (34) and simplifying ρ:

$$\vec{u}\cdot\left(\frac{\nabla T}{T} + \frac{\gamma-1}{2}\mathrm{Ma}^2\frac{\nabla u^2}{u^2} - \frac{\nabla q}{c_pT}\right) = 0 \tag{36}$$

Notice that by developing the scalar product $\vec{u}\cdot\nabla(\,)$ it follows that

$$\cancel{u_r}\frac{\partial(\,)}{\partial r} + \frac{u_\theta}{r}\cancel{\frac{\partial(\,)}{\partial\theta}} + u_z\frac{\partial(\,)}{\partial z} \tag{37}$$

where some terms are canceled out due to the previous hypotheses. It follows that only the axial component of the product is non-null. Therefore, since it is equal to 0, it is possible to simplify u_z and obtain the following equation:

$$\frac{dT}{T} + \frac{\gamma-1}{2}\mathrm{Ma}^2\frac{du^2}{u^2} - \frac{dq}{c_pT} = 0 \qquad or \qquad dh + dk - dq = 0 \tag{38}$$

The ratio Ma^2/u^2 is the sound velocity, and thus – using the identity of Eq. (8) – the following equalities are true:

$$\mathrm{Ma}^2\frac{du^2}{u^2} = \mathrm{Ma}^2\frac{du_z^2 + du_\theta^2}{u^2} = \mathrm{Ma}^2\frac{du_z^2}{u^2} + \mathrm{Ma}^2\frac{du_\theta^2}{u^2} = \mathrm{Ma}_z^2\frac{du_z^2}{u_z^2} + \mathrm{Ma}_\theta^2\frac{du_\theta^2}{u_\theta^2} \tag{39}$$

Hence, Eq. (38) can also be written as follows:

$$\frac{dq}{c_pT} = \frac{dT}{T} + \frac{\gamma-1}{2}\left(\mathrm{Ma}_z^2\frac{du_z^2}{u_z^2} + \mathrm{Ma}_\theta^2\frac{du_\theta^2}{u_\theta^2}\right) \tag{40}$$

Summary of the results

Equations (17), (21), (30) and (40) have been expressed along the axial direction. The same is immediate for equations (5), (7), (11) and (14), where it is sufficient to retain the axial component from the gradient. All the aforementioned equations are collected on the right side of Table 1. On the left side, the same equations derived by Shapiro [4] at comparison. From Tab. 1 it can be observed that:

- Perfect gas, sonic velocity and entropy equations are invariant in the presence or absence of swirl.
- The differential equation of the mach number is still valid for the magnitude of the mach number as well for every single component.
- The mass equation is specific for the axial component of the velocity.
- The energy equation takes into account the kinetic energy, thus both the axial and tangential velocities appear.
- The momentum equation is specific for the axial component of the velocity, while a new relation for the tangential component of the velocity appears from the conservation of vorticity.
- Vorticity is null for 1D flows, as well as the tangential velocity. For 1D flows, both the vorticity equation and the tangential mach number equation are not valid, and the other new equations collapse in the Shapiro's equations.

DOI: 10.13009/EUCASS2025-437

Table 1: The Shapiro's differential equations for 1D flows (left) and the new differential equations with swirl for quasi-1D flows (right), with $d = \partial(\,)/\partial z$ and the tangential components are r and z functions: $u_\theta = u_\theta(z, r)$, $\mathrm{Ma}_\theta = \mathrm{Ma}_\theta(z, r)$.

Derivation	**Shapiro**	**with Swirl**	**Eq. reference**
perfect gas	$\frac{dp}{p} = \frac{d\rho}{\rho} + \frac{dT}{T} + \frac{dR}{R}$	$\frac{dp}{p} = \frac{d\rho}{\rho} + \frac{dT}{T} + \frac{dR}{R}$	(5)
sonic velocity	$\frac{da}{a} = \frac{1}{2}\left(\frac{d\gamma}{\gamma} + \frac{dT}{T} + \frac{dR}{R}\right)$	$\frac{da}{a} = \frac{1}{2}\left(\frac{d\gamma}{\gamma} + \frac{dT}{T} + \frac{dR}{R}\right)$	(7)
Mach number	$\frac{d\mathrm{Ma}^2}{\mathrm{Ma}^2} = \frac{du^2}{u^2} - \frac{dR}{R} - \frac{d\gamma}{\gamma} - \frac{dT}{T}$	$\frac{d\mathrm{Ma}_z^2}{\mathrm{Ma}_z^2} = \frac{du_z^2}{u_z^2} - \frac{dR}{R} - \frac{d\gamma}{\gamma} - \frac{dT}{T}$	(11)
		$\frac{d\mathrm{Ma}_\theta^2}{\mathrm{Ma}_\theta^2} = \frac{du_\theta^2}{u_\theta^2} - \frac{dR}{R} - \frac{d\gamma}{\gamma} - \frac{dT}{T}$	(11)
mass	$\frac{d\rho}{\rho} + \frac{dA}{A} + \frac{du}{u} = 0$	$\frac{d\rho}{\rho} + \frac{dr^2}{r^2} + \frac{du_z}{u_z} = 0$	(17)
energy	$\frac{dq}{c_pT} = \frac{dT}{T} + \frac{\gamma-1}{2}\mathrm{Ma}^2\frac{du^2}{u^2}$	$\frac{dq}{c_pT} = \frac{dT}{T} + \frac{\gamma-1}{2}\left(\mathrm{Ma}_z^2\frac{du_z^2}{u_z^2} + \mathrm{Ma}_\theta^2\frac{du_\theta^2}{u_\theta^2}\right)$	(40)
momentum	$\frac{dp}{p} + \frac{1}{2}\gamma\mathrm{Ma}^2\frac{du^2}{u^2} = 0$	$\frac{dp}{p} + \frac{1}{2}\gamma\mathrm{Ma}_z^2\frac{du_z^2}{u_z^2} = 0$	(21)
		$\frac{dr}{r} + \frac{du_\theta}{u_\theta} = 0$	(30)
entropy	$\frac{ds}{c_p} = \frac{dT}{T} - \frac{\gamma-1}{\gamma}\frac{dp}{p}$	$\frac{ds}{c_p} = \frac{dT}{T} - \frac{\gamma-1}{\gamma}\frac{dp}{p}$	(14)

3. Results and Discussion

3.1 General Quasi-1D Differential Equations: matrix form

Following Shapiro layout, the found differential equations can be rearranged as:

$$d\vec{y} = \mathbf{M}\, d\vec{x} \tag{41}$$

where $\vec{x}$ are the independent variables

$$d\vec{x} = \begin{bmatrix} \dfrac{dr^2}{r^2} & \dfrac{dq}{c_pT} & \dfrac{dR}{R} & \dfrac{d\gamma}{\gamma} \end{bmatrix} \tag{42}$$

and $\vec{y}$ are the dependent variables

$$d\vec{y} = \begin{bmatrix} \dfrac{d\mathrm{Ma}_z^2}{\mathrm{Ma}_z^2} & \dfrac{d\mathrm{Ma}_\theta^2}{\mathrm{Ma}_\theta^2} & \dfrac{du_z^2}{u_z^2} & \dfrac{du_\theta^2}{u_\theta^2} & \dfrac{da}{a} & \dfrac{dT}{T} & \dfrac{d\rho}{\rho} & \dfrac{dp}{p} & \dfrac{ds}{c_p} \end{bmatrix} \tag{43}$$

and $\mathbf{M}$ is the relation matrix function of only γ, Ma_z and Ma_θ. How to derive $\mathbf{M}$ is shown in Appendix A. The whole matrix $\mathbf{M}$ takes the form of

$$\mathbf{M} = \begin{bmatrix} -2\frac{1+\frac{\gamma-1}{2}\mathrm{Ma}_z^2}{1-\mathrm{Ma}_z^2} + \frac{1+\gamma\mathrm{Ma}_z^2}{1-\mathrm{Ma}_z^2}S & \frac{1+\gamma\mathrm{Ma}_z^2}{1-\mathrm{Ma}_z^2} & \frac{1+\gamma\mathrm{Ma}_z^2}{1-\mathrm{Ma}_z^2} & -1 \\ -\frac{1+(\gamma-2)\mathrm{Ma}_z^2}{1-\mathrm{Ma}_z^2} - \frac{1-\gamma\mathrm{Ma}_z^2}{1-\mathrm{Ma}_z^2}S & -\frac{1-\gamma\mathrm{Ma}_z^2}{1-\mathrm{Ma}_z^2} & -\frac{1-\gamma\mathrm{Ma}_z^2}{1-\mathrm{Ma}_z^2} & -1 \\ -\frac{1}{1-\mathrm{Ma}_z^2} + \frac{1}{1-\mathrm{Ma}_z^2}S & \frac{1}{1-Ma_z^2} & \frac{1}{1-Ma_z^2} & 0 \\ -\frac{1}{2} & 0 & 0 & 0 \\ \frac{(\gamma-1)\mathrm{Ma}_z^2}{2\left(1-\mathrm{Ma}_z^2\right)} + \frac{1-\gamma\mathrm{Ma}_z^2}{2(1-\mathrm{Ma}_z^2)}S & \frac{1-\gamma\mathrm{Ma}_z^2}{2\left(1-\mathrm{Ma}_z^2\right)} & \frac{1-\gamma\mathrm{Ma}_z^2}{2\left(1-\mathrm{Ma}_z^2\right)} & \frac{1}{2} \\ \frac{(\gamma-1)Ma_z^2}{1-\mathrm{Ma}_z^2} + \frac{1-\gamma\mathrm{Ma}_z^2}{1-\mathrm{Ma}_z^2}S & \frac{1-\gamma\mathrm{Ma}_z^2}{1-\mathrm{Ma}_z^2} & \frac{(1-\gamma)\mathrm{Ma}_z^2}{1-\mathrm{Ma}_z^2} & 0 \\ \frac{\mathrm{Ma}_z^2}{1-\mathrm{Ma}_z^2} - \frac{1}{1-\mathrm{Ma}_z^2}S & -\frac{1}{1-Ma_z^2} & -\frac{1}{1-Ma_z^2} & 0 \\ \frac{\gamma\mathrm{Ma}_z^2}{1-\mathrm{Ma}_z^2} - \frac{\gamma\mathrm{Ma}_z^2}{1-\mathrm{Ma}_z^2}S & -\frac{\gamma\mathrm{Ma}_z^2}{1-\mathrm{Ma}_z^2} & -\frac{\gamma\mathrm{Ma}_z^2}{1-\mathrm{Ma}_z^2} & 0 \\ S & 1 & 0 & 0 \end{bmatrix} \tag{44}$$

where $S \doteq \mathrm{Ma}_\theta^2(\gamma - 1)/2$. Observe that the matrix can be split as the two contributes defined by the presence or not of the swirl, by defining $\mathbf{M}_0$ the Shapiro's matrix – no swirl – and $\mathbf{M}_S$ the new terms associated to swirl. The two matrices are coupled by the following relation and defined as follows:

$$d\vec{y} = (\mathbf{M}_0 + \mathbf{M}_S\, S\,)\, d\vec{x} \tag{45}$$

DOI: 10.13009/EUCASS2025-437

where

$$\mathbf{M}_0 = \begin{bmatrix} -2\frac{1+\frac{\gamma-1}{2}\mathrm{Ma}_z^2}{1-\mathrm{Ma}_z^2} & \frac{1+\gamma\mathrm{Ma}_z^2}{1-\mathrm{Ma}_z^2} & \frac{1+\gamma\mathrm{Ma}_z^2}{1-\mathrm{Ma}_z^2} & -1 \\ -\frac{1+(\gamma-2)\mathrm{Ma}_z^2}{1-\mathrm{Ma}_z^2} & -\frac{1-\gamma\mathrm{Ma}_z^2}{1-\mathrm{Ma}_z^2} & -\frac{1-\gamma\mathrm{Ma}_z^2}{1-\mathrm{Ma}_z^2} & -1 \\ -\frac{1}{1-\mathrm{Ma}_z^2} & \frac{1}{1-Ma_z^2} & \frac{1}{1-Ma_z^2} & 0 \\ -\frac{1}{2} & 0 & 0 & 0 \\ \frac{(\gamma-1)\mathrm{Ma}_z^2}{2(1-\mathrm{Ma}_z^2)} & \frac{1-\gamma\mathrm{Ma}_z^2}{2(1-\mathrm{Ma}_z^2)} & \frac{1-\gamma\mathrm{Ma}_z^2}{2(1-\mathrm{Ma}_z^2)} & \frac{1}{2} \\ \frac{(\gamma-1)Ma_z^2}{1-\mathrm{Ma}_z^2} & \frac{1-\gamma\mathrm{Ma}_z^2}{1-\mathrm{Ma}_z^2} & \frac{(1-\gamma)\mathrm{Ma}_z^2}{1-\mathrm{Ma}_z^2} & 0 \\ \frac{\mathrm{Ma}_z^2}{1-\mathrm{Ma}_z^2} & -\frac{1}{1-Ma_z^2} & -\frac{1}{1-Ma_z^2} & 0 \\ \frac{\gamma\mathrm{Ma}_z^2}{1-\mathrm{Ma}_z^2} & -\frac{\gamma\mathrm{Ma}_z^2}{1-\mathrm{Ma}_z^2} & -\frac{\gamma\mathrm{Ma}_z^2}{1-\mathrm{Ma}_z^2} & 0 \\ 0 & 1 & 0 & 0 \end{bmatrix} \quad \mathbf{M}_S = \begin{bmatrix} \frac{1+\gamma\mathrm{Ma}_z^2}{1-\mathrm{Ma}_z^2} & 0 & 0 & 0 \\ -\frac{1-\gamma\mathrm{Ma}_z^2}{1-\mathrm{Ma}_z^2} & 0 & 0 & 0 \\ \frac{1}{1-\mathrm{Ma}_z^2} & 0 & 0 & 0 \\ 0 & 0 & 0 & 0 \\ \frac{1-\gamma\mathrm{Ma}_z^2}{2(1-\mathrm{Ma}_z^2)} & 0 & 0 & 0 \\ \frac{1-\gamma\mathrm{Ma}_z^2}{1-\mathrm{Ma}_z^2} & 0 & 0 & 0 \\ -\frac{1}{1-\mathrm{Ma}_z^2} & 0 & 0 & 0 \\ -\frac{\gamma\mathrm{Ma}_z^2}{1-\mathrm{Ma}_z^2} & 0 & 0 & 0 \\ 1 & 0 & 0 & 0 \end{bmatrix} \tag{46}$$

Both matrices are only function of axial mach number and specific heat. The scalar S is the dynamic tangential mach temperature, and if null the total matrix $\mathbf{M}$ coincides with $\mathbf{M}_0$, that is Shapiro original matrix.

3.2 Convergent: Throat Area Reduction due to Swirl

Let's consider for simplicity an adiabatic nozzle and constant specific heat and gas constant: $q = 0$, $d\gamma = 0$, $dR = 0$. Consider as well that the radius of interest it the wall radius, $r = R$. By doing so, the only independent remaining variable in Eq. (45) is the nozzle area section $dr^2 = dR^2 = dA$. Following plot in Fig. 1 (left) shows the convergence ratio – A_c/A_t – to pass from an axial mach number of 0.01 to axial sonic conditions, for different values of Ma_θ at the throat and wall. The adjacent Fig. 1 (right) plots the axial evolution of the correspondent tangential mach number at wall. Figure 2 shows the evolution of their ratio.

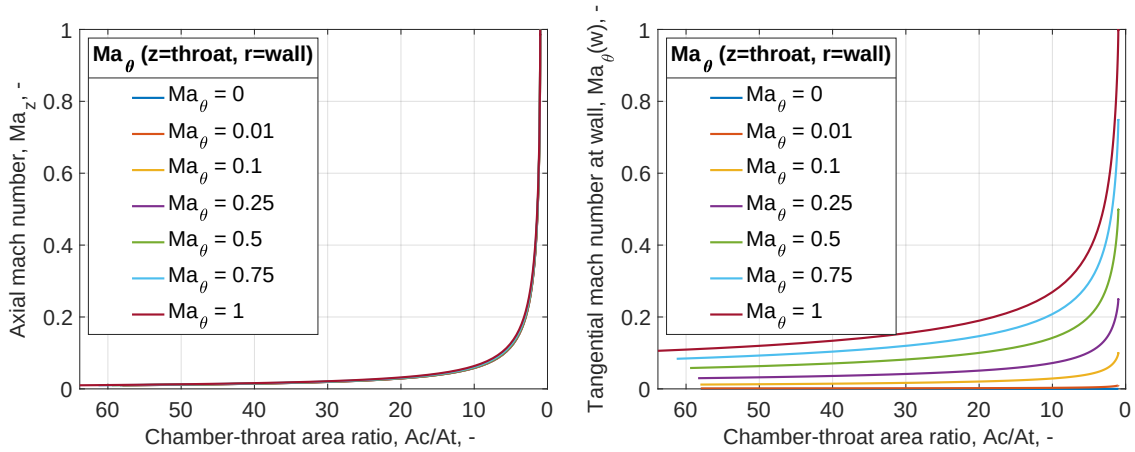

Figure 1: Axial mach number (left) and tangential mach number at the wall (right) as function of the chamber-throat area ratio, for different tangential mach number at the wall at throat

The presence of swirl slows down the acceleration of the axial velocity. In the showed figures, this is highlighted by higher contraction ratios (left part of the plots, around $A_c/A_t = 60$) required to reach $\mathrm{Ma}_z = 1$ at throat. When the combustion chamber section is fixed, it follows that the flow needs to contract more with respect to the throat area associated to a only-axial expansion. The consequence is a reduction of the throat section function of Ma_θ wall reached at the throat, as showed in Fig. 3. An approximating equation for the relation in Fig. 3 is given by the following 2nd-order polynomial:

$$\eta_A = 1.000 - 0.008\,\mathrm{Ma}_\theta\,|_{w,th} - 0.085\,\mathrm{Ma}_\theta^2\,|_{w,th} \qquad R^2 = 0.999 \tag{47}$$

where the mach number can be replaced with the mach number ratio since the axial mach number is 1 at throat. The presence of swirl therefore affects the characteristic velocity, which equation becomes:

$$c^* = \frac{p_c\,A_t\,\eta_A}{\dot{m}} = c^*_{no\ swirl}\,\eta_A \tag{48}$$

DOI: 10.13009/EUCASS2025-437

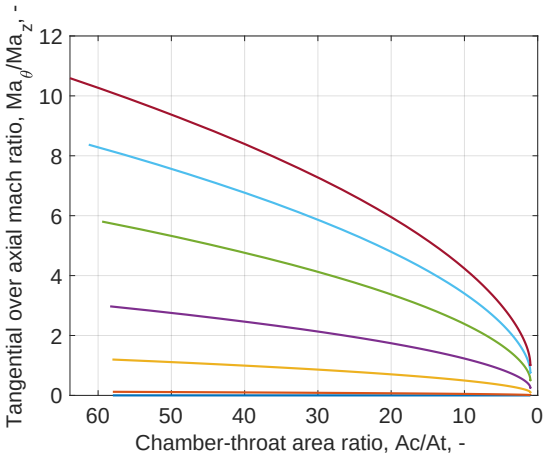

Figure 2: Tangential (at wall) over axial mach number as function of the chamber-throat area ratio for different tangential mach number at the wall at throat

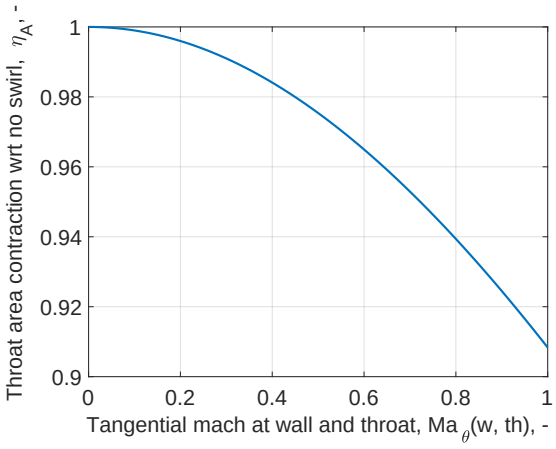

Figure 3: Throat area reduction wrt no swirl function of the tangential mach number at wall reached at throat

3.3 Divergent

Figures 4 and 5 shows the behavior in the divergent part of the nozzle up to an expansion ratio of 4.

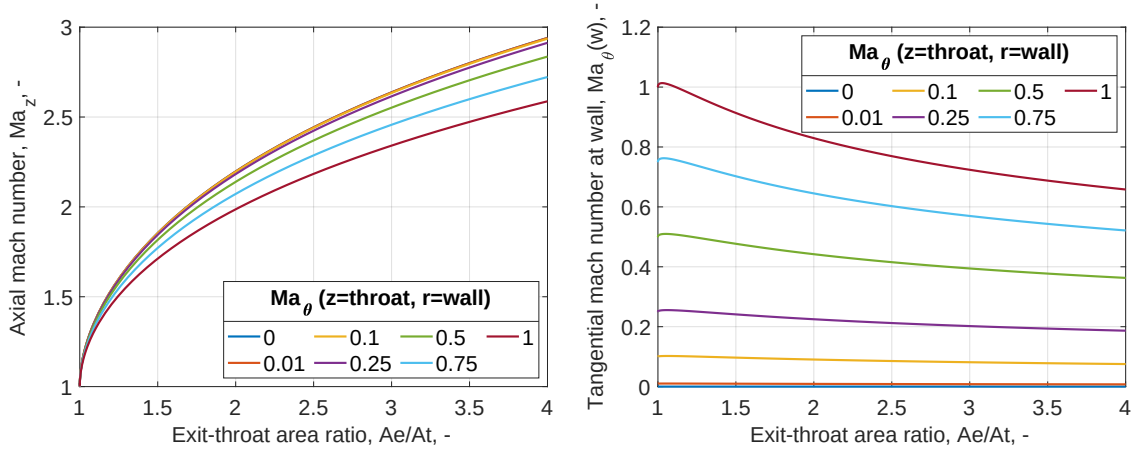

Figure 4: Axial mach number (left) and tangential mach number at the wall (right) as function of the exit-throat area ratio, for different tangential mach number at the wall at throat

DOI: 10.13009/EUCASS2025-437

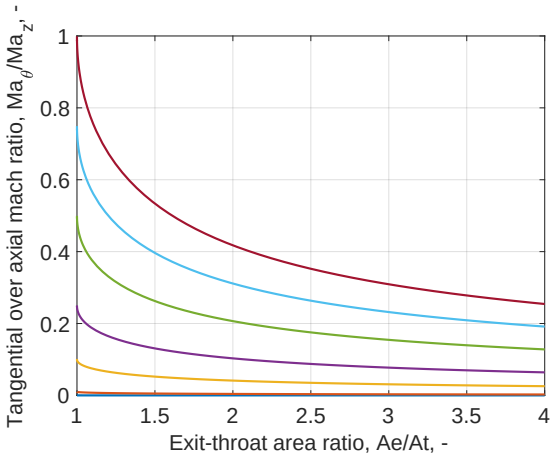

Figure 5: Tangential (at wall) over axial mach number as function of the exit-throat area ratio for different tangential mach number at the wall at throat

The same previous discussion holds. The tangential mach number slightly decreases as a result of the increase of the section. The axial mach number grows is slowed by the presence of swirl. This affects the exit velocity thus the thrust, that therefore is going to be reduced with respect to the fully-axial flow. This result can be implemented to improve proposed model of Santolini et al. [6] by:

1. substituting Shapiro's model with the model proposed in this paper
2. replacing the throat area corrective factor with the tangential velocity at wall (wherever).

By doing that, the experimental measure of thrust would allow to compute the unknown swirl entering (or exiting) the nozzle and thus compute the correct experimental c^* with the use of Eq. (48).

3.4 The Swirl Number

Let's now introduce the swirl number, as ratio between the axial flux of angular momentum and axial flux of axial momentum normalized respect to the duct radius [26–29].

$$Sw(z) = \frac{1}{R}\frac{G_\theta}{G_z} \tag{49}$$

with

$$G_\theta = 2\pi \int_0^R \rho u_\theta(r) u_z r^2 dr = 2\pi\rho u_z \int_0^R u_\theta(r)\, r^2 dr \tag{50}$$

and

$$G_z = 2\pi \int_0^R \rho u_z^2 r\, dr = \pi\rho u_z^2 R^2 \tag{51}$$

Therefore, it follows that:

$$Sw(z) = \frac{2}{R^3}\frac{\int_0^R u_\theta(r)\, r^2 dr}{u_z} \tag{52}$$

Latter equation can be rearranged with a change of variable $\zeta \doteq r/R$ as:

$$Sw(z) = 2\frac{\int_0^1 u_\theta(\zeta)\, \zeta^2 d\zeta}{u_z} \tag{53}$$

Now, by defining the tangential velocity radial profile as function of its normalized profile:

$$u_\theta(\zeta) \doteq u_\theta(w) f_{u_\theta}(\zeta) \tag{54}$$

where for example $f(\zeta) = \zeta = r/R$ for the solid-body type rotation, it follows that:

$$Sw(z) = \frac{u_\theta(w)}{u_z} \cdot \left(2\int_0^1 f(\zeta)\, \zeta^2 d\zeta\right) \tag{55}$$

DOI: 10.13009/EUCASS2025-437

Since the result of the operation inside the brackets is constant, and the velocities ratio is equal to the mach ratios, it follows:

$$S\,w\,(z) \propto \frac{\mathrm{Ma}_\theta\,|_w}{\mathrm{Ma}_z} \tag{56}$$

or $S\,w\,(z) = \mathrm{Ma}_\theta\,|_w\,/(2\,\mathrm{Ma}_z)$ for the solid-body profile.
The relation of Eq. (56) states that the swirl number develops proportionally to the tangential-axial mach ratio. The swirl decays through the nozzle in the same way pictured in Fig. 2. In the plotted example, the decrement is of a factor $\sim$ 10–12 to pass from $\mathrm{Ma}_z = 0.01$ to $\mathrm{Ma}_z = 1$.

4. CFD comparison

The analytical model was tested on the data from a CFD simulation of the VFP at SPLab, an hybrid rocket engine characterized by fully-tangential oxidizer injection. Figure 6 (left) is a picture of the nozzle-convergent side after a firing test. The swirling traces left by the soot can be noticed. On the right side, the mach lines in the nozzle result of the CFD simulation.

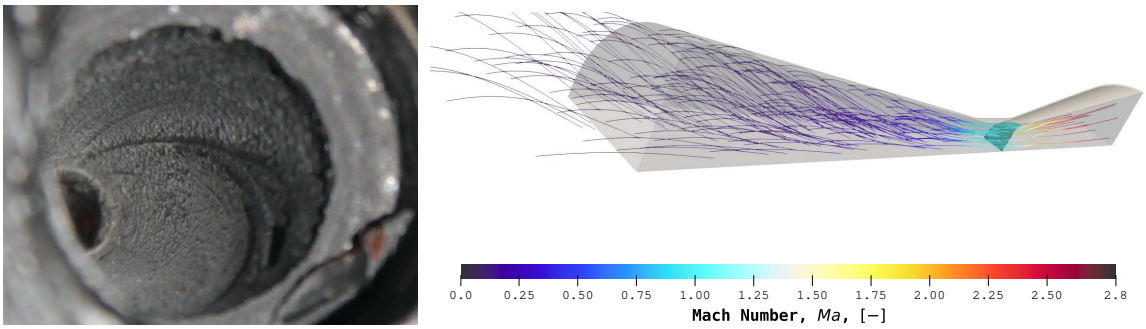

Figure 6: VFP nozzle swirl line traces after a firing test (left) and mach lines from CFD (right)

CFD data were useful to verify that the axial velocity profile along the radius is constant as assumed by the hypothesis, $\mathrm{Ma}_z(r) = \overline{\mathrm{Ma}_z}$. In addition – even if it is not a requirement for the analytical model – the radial profile of the tangential velocity was compared with a solid-body profile, $\mathrm{Ma}_\theta(r) = \mathrm{Ma}_\theta\,|_W \cdot r/R$. The fitting data in different A/A_t ratios are reported with their evaluation quality criteria for the fitting in Tab. 2.

Table 2: From left to right: 1) area-throat area ratio (convergent-throat-divergent), 2) tangential mach at wall, 3) R^2 for solid-body profile assumption, 4) mean axial mach, 5) standard deviation for constant profile assumption

$\mathbf{A/A_t}$	$\mathbf{Ma_\theta\,|_W}$	$\mathbf{R^2}$	$\mathbf{\overline{Ma_z}}$	**std**
12.2	0.038	0.953	0.047	0.003
12.2	0.035	0.948	0.046	0.003
12.2	0.033	0.949	0.046	0.002
12.2	0.031	0.950	0.047	0.002
12.2	0.031	0.941	0.051	0.000
9.7	0.033	0.943	0.064	0.001
7.5	0.036	0.942	0.085	0.002
5.6	0.041	0.948	0.115	0.003
3.9	0.047	0.955	0.162	0.003
2.6	0.056	0.962	0.249	0.004
1.5	0.072	0.969	0.449	0.005
1.0	0.091	0.967	0.968	0.002
1.4	0.100	0.781	1.639	0.022
2.6	0.079	0.714	2.194	0.025
4.2	0.069	0.713	2.632	0.003

The quasi-1D model was integrated from throat to chamber section and then from throat to exit section to avoid numerical instabilities. Initial mach conditions are taken from the row of Tab. 2 for $A/A_t = 1$. An adiabatic system was considered both in CFD and the model. However, the model was also run at constant $\gamma = 1.33$ and constant R for

DOI: 10.13009/EUCASS2025-437

simplicity. Figures 7, 8 and 9 shows the result compared with the CFD data respectively for the axial, tangential, and tangential-over-axial mach numbers, with convergent on the left and divergent on the right.

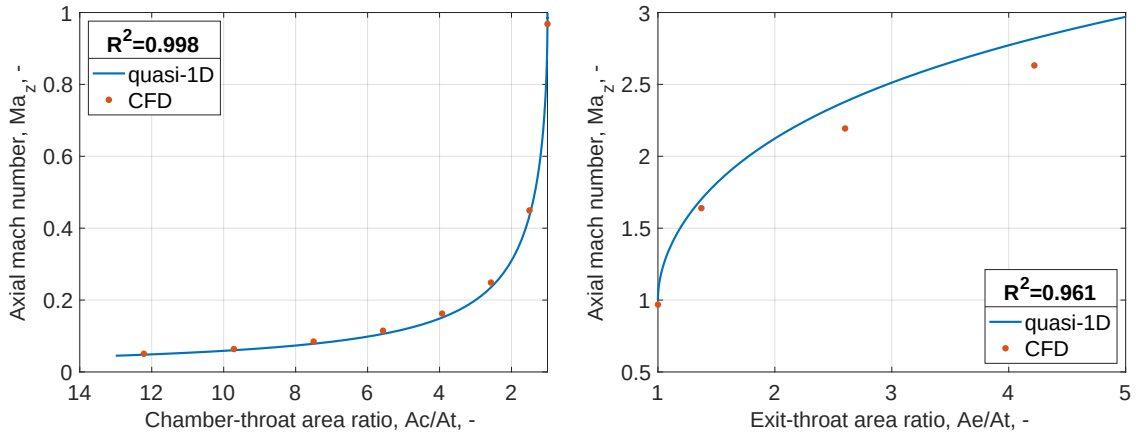

Figure 7: Convergent (left) and divergent (right) quasi-1D compared with CFD data: axial mach number

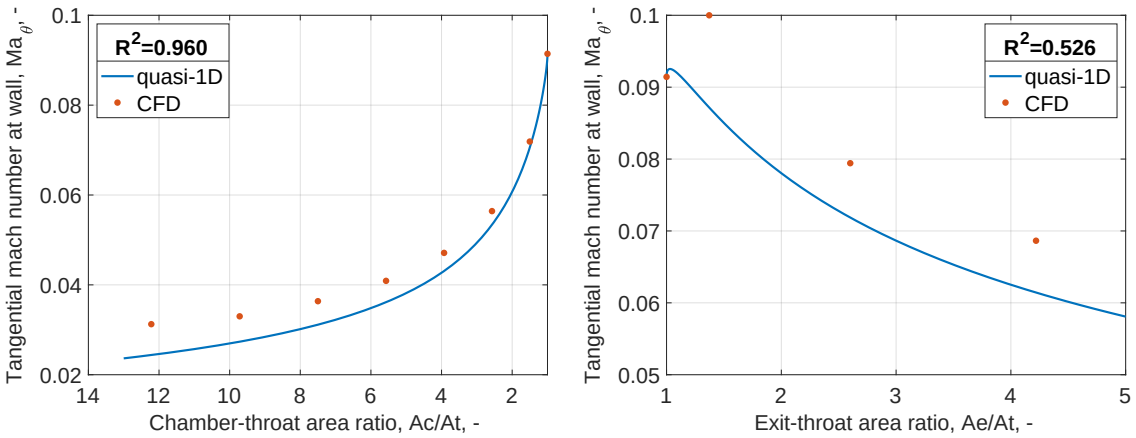

Figure 8: Convergent (left) and divergent (right) quasi-1D compared with CFD data: tangential mach number at wall

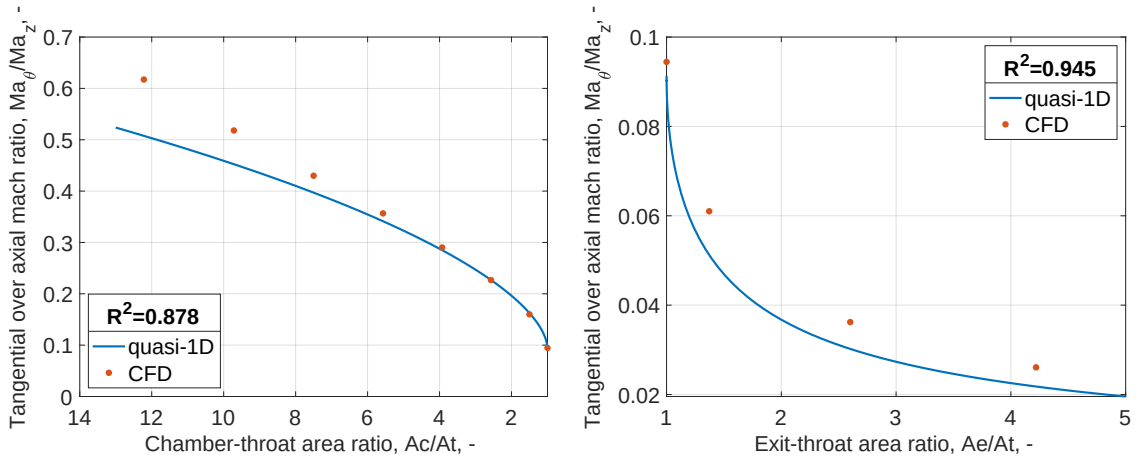

Figure 9: Convergent (left) and divergent (right) quasi-1D compared with CFD data: tangential-axial mach ratio

DOI: 10.13009/EUCASS2025-437

The quasi-1D model fits well the CFD data, with high R^2 despite the constant γ and R. The divergent tangential mach number in Fig. 8 (right) is the worst case, but it is probably due to complex 3D interactions that arise from the nozzle geometry (see Fig. 6 right). Indeed, the smooth change in area – one of the hypotheses behind the quasi-1D model – is respected in the convergent and divergent. However, at the edges of the throat there is a discontinuity causing mismatch between the two dataset. Furthermore, the nozzle throat is built as a short length at constant section. Mathematically, for the quasi-1D model it means constant properties, but for the CFD it causes complex interactions due to the combined effects of supersonic speeds in a narrow channel, the flow viscosity, and the interaction with the boundary layer.

5. Conclusions

This work presents a new quasi-1D analytical model to describe the propagation of swirl in rocket nozzles, extending the classical Shapiro differential equations to account for tangential velocity components and vorticity conservation.
The model demonstrates that the presence of swirl leads to an apparent contraction of the nozzle throat area as expected from different experimental observations in the literature, which, if unaccounted for, can result in an overestimation of combustion efficiency. To correct for this, a second-order polynomial correction factor was introduced as function of the tangential Mach number at the wall at throat, enabling for more accurate calculation of the characteristic velocity in swirled flows. The correction factor can go from unity for no swirl to ~ 0.91 for sonic tangential mach numbers. The swirl number was analytically linked to the ratio of tangential to axial Mach numbers, providing insight into its evolution along the nozzle. Numerical integration of the model shows that the tangential Mach number increases from the combustion chamber toward the nozzle throat, reducing the expected swirl decay in the converging section. As a result, even a low initial swirl in the chamber can still cause a non-negligible throat contraction.
The model was validated through a CFD simulation of the Vortex Flow Pancake (VFP) engine, demonstrating strong agreement in both axial and tangential Mach number predictions. The CFD simulation also demonstrated that uniform axial and solid-body tangential velocities are a good approximation along the radial direction of a nozzle. While the model performs well under the assumptions of axisymmetry and smooth nozzle geometry, minor discrepancies were observed at the throat, attributed to three-dimensional effects and geometric discontinuities.
Overall, the proposed model offers a reliable and physically consistent alternative to existing correction methods and is suitable for improving the accuracy of combustion efficiency evaluations in rocket engines operating with swirling flows.

References

[1] C. Goldman and A. Gany. 1996. Thrust modulation of ram-rockets by a vortex valve. In: *32nd Joint Propulsion Conference & Exhibit*. DOI: 10.2514/6.1996-2624.

[2] A. Gany, M. Mor, and C. Goldman. 2005. Analysis and characteristics of choked swirling nozzle flows. *AIAA Journal*. 43:2177–2181. DOI: 10.2514/1.16887.

[3] G. Haag. 2001. Alternative geometry hybrid rockets for spacecraft orbit transfer. PhD Thesis. University of Surrey (UK).

[4] A. Shapiro. *The Dynamics and Thermodynamics of Compressible Fluid Flow*. 1953. John Wiley & Sons.

[5] V. Santolini, R. Bisin, F. Giambelli, and C. Paravan. 2023. An overview of splab activities on vortex combustion in a non-conventional hybrid rocket engine. In: *The Thirteenth International Symposium on Special Topics in Chemical Propulsion and Energetic Materials (13-ISICP)*.

[6] V. Santolini and C. Paravan. 2024. Innovative methodology for evaluating combustion efficiency in swirled rocket engines. In: *IAF Space Propulsion Symposium (75th International Astronautical Congress)*. 1040–1052.

[7] N. Bellomo, F. Barato, F. Faenza, M. Lazzarin, A. Bettella, and D. Pavarin. 2013. Numerical and experimental investigation of unidirectional vortex injection in hybrid rocket engines. *Journal of Propulsion and Power*. 29:1097–1113. DOI: 10.2514/1.B34506.

[8] I. Nakagawa, D. Kishizato, Y. Koinuma, and S. Tanaka. 2021. Demonstration of an altering-intensity swirling-oxidizer-flow-type hybrid rocket function. *Journal of Propulsion and Power*. 37:326–331. DOI: 10.2514/1.B37915.

[9] W. Knuth, M. Chiaverini, D. Gramer, and J. Sauer. 1998. Experimental investigation of a vortex-driven high-regression rate hybrid rocket engine. In: *34th AIAA/ASME/SAE/ASEE Joint Propulsion Conference & Exhibit*. DOI: 10.2514/6.1998-3348.

DOI: 10.13009/EUCASS2025-437

[10] W. Knuth, M. Chiaverini, D. Gramer, and J. Sauer. 1998. Development and testing of a vortex-driven, high-regression rate hybrid rocket engine. In: *34th AIAA/ASME/SAE/ASEE Joint Propulsion Conference & Exhibit*. DOI: 10.2514/6.1998-3507.

[11] W. Knuth, M. Chiaverini, J. Sauer, and D. Gramer. 2002. Solid-fuel regression rate behavior of vortex hybrid rocket engines. *Journal of Propulsion and Power*. 18:600–609. DOI: 10.2514/2.5974.

[12] S. Yuasa, N. Shiraishi, and K. Hirata. 2012. Controlling parameters for fuel regression rate of swirling-oxidizer-flow-type hybrid rocket engine. In: *48th AIAA/ASME/SAE/ASEE Joint Propulsion Conference & Exhibit*. DOI: 10.2514/6.2012-4106.

[13] B. Vignesh and R. Kumar. 2020. Effect of multi-location swirl injection on the performance of hybrid rocket motor. *Acta Astronautica*. 176:111–123. DOI: 10.1016/j.actaastro.2020.06.029.

[14] D. Gibbon and G. Haag. 2001. Investigation of an alternative geometry hybrid rocket for small spacecraft orbit transfer. *Surrey Satellite Technology LTD Guildford (UK)*.

[15] A. Hashish, C. Paravan, and A. Verga. 2021. Liquefying fuel combustion in a lab-scale vortex flow pancake hybrid rocket engine. In: *AIAA Propulsion and Energy 2021 Forum*. DOI: 10.2514/6.2021-3519.

[16] A. Mager. 1961. Approximate solution of isentropic swirling flow through a nozzle. *ARS Journal*. 31:1140–1148. DOI: 10.2514/8.5732.

[17] A. D. Cutler and R. W. Barnwell. 1999. Vortex flow in a convergent-divergent nozzle. *AIAA Journal*. 37:1329–1331. DOI: 10.2514/2.606.

[18] A. Abdelhafez and A. Gupta. 2010. Swirling airflow through a nozzle: choking criteria. *Journal of Propulsion and Power*. 26:754–764. DOI: 10.2514/1.47956.

[19] S. Yuasa, N. Shiraishi, M. Sakamoto, C. Sezaki, K. Hirata, and T. Sakurai. 2011. Evaluation method of c* efficiency of swirling-oxidizer-flow-type hybrid rocket engines. *Japan Society of Aeronautical Space Sciences*. 59:97–101. DOI: 10.2322/jjsass.59.97.

[20] K. Ozawa, K. Kitagawa, S. Aso, and T. Shimada. 2019. Hybrid rocket firing experiments at various axial–tangential oxidizer-flow-rate ratios. *Journal of Propulsion and Power*. 35:94–108. DOI: 10.2514/1.B36889.

[21] W. Lewellen, W. Burns, and H. Strickland. 1969. Transonic swirling flows. *AIAA Journal*. 7:1290–1297.

[22] T. Gillespie and J. Shearer. 1972. The control of thrust and flow rate in choked nozzles by vortex generation. *Fluidics Quarterly*. 4:50–55.

[23] A. Cutler and R. Barnwell. 1999. Vortex flow in a convergent–divergent nozzle. *AIAA Journal*. 37:1329–1331.

[24] J. Batson and R. Sforzini. 1970. Swirling flow through a nozzle. *Journal of Spacecraft and Rockets*. 7:159–163.

[25] D. Norton, B. Farquhar, and J. Hoffman. 1969. An analytical and experimental investigation of swirling flows in nozzles. *AIAA Journal*. 7:1992–2000.

[26] G. Vignat, D. Durox, and S. Candel. 2022. The suitability of different swirl number definitions for describing swirl flows: accurate, common and (over-) simplified formulations. *Progress in Energy and Combustion Science*. 89:100969. DOI: 10.1016/j.pecs.2021.100969.

[27] R. Sharma and M. Kumar. 2023. Characterizing swirl strength and recirculation zone formation in tangentially injected isothermal flows. *Journal of Applied Fluid Mechanics*. 16:549–560.

[28] N. Syred and J. Beér. 1974. Combustion in swirling flows: a review. *Combustion and flame*. 23:143–201.

[29] A. Gupta, D. Lilley, and N. Syred. *Swirl flows*. 1984. Tunbridge Wells, Kent, England, Abacus Press.

DOI: 10.13009/EUCASS2025-437

A. The Arithmetic behind the New Matrix

Let's drop the denominators – that are used for normalized results – to lighten the notation in the following arithmetic.

Matrix row 1

From (11) and substituting

$$
\begin{aligned}
d\mathrm{Ma}_z^2 &= du_z^2 - dT - d\gamma - dR \\
&\quad but \quad dT = dq - \frac{\gamma-1}{2}\mathrm{Ma}_z^2\, du_z^2 - \frac{\gamma-1}{2}\mathrm{Ma}_\theta^2\, du_\theta^2 \quad from\ (40) \Rightarrow \\
&= du_z^2 - dq + \frac{\gamma-1}{2}\mathrm{Ma}_z^2\, du_z^2 + \frac{\gamma-1}{2}\mathrm{Ma}_\theta^2\, du_\theta^2 - d\gamma - dR \\
&= \left(1 + \frac{\gamma-1}{2}\mathrm{Ma}_z^2\right) du_z^2 + \frac{\gamma-1}{2}\mathrm{Ma}_\theta^2\, du_\theta^2 - dq - d\gamma - dR
\end{aligned}
\tag{57}
$$

From mass Eq. (17)

$$
\begin{aligned}
du_z^2 &= -2(dr^2 + d\rho) \\
&\quad but \quad d\rho = dp - dT - dR \quad from\ (5) \Rightarrow \\
&= -2(dr^2 + dp - dT - dR) \\
&\quad but \quad dp = -\frac{1}{2}\gamma\mathrm{Ma}_z^2\, du_z^2 \quad from\ (21) \Rightarrow \\
&= -2(dr^2 - \frac{1}{2}\gamma\mathrm{Ma}_z^2\, du_z^2 - dq + \frac{\gamma-1}{2}\mathrm{Ma}_z^2\, du_z^2 + \frac{\gamma-1}{2}\mathrm{Ma}_\theta^2\, du_\theta^2 - dR) \\
&= -2dr^2 + \gamma\mathrm{Ma}_z^2\, du_z^2 + 2dq - (\gamma-1)\mathrm{Ma}_z^2\, du_z^2 - (\gamma-1)\mathrm{Ma}_\theta^2\, du_\theta^2 + 2dR \\
&= \frac{-2dr^2 + 2dq + 2dR - (\gamma-1)\mathrm{Ma}_\theta^2\, du_\theta^2}{1 - \mathrm{Ma}_z^2}
\end{aligned}
\tag{58}
$$

Thus, by substituting Eq. (58) in Eq.(57):

$$
\begin{aligned}
d\mathrm{Ma}_z^2 &= \left(1 + \frac{\gamma-1}{2}\mathrm{Ma}_z^2\right)\frac{-2dr^2 + 2dq + 2dR - (\gamma-1)\mathrm{Ma}_\theta^2\, du_\theta^2}{1 - \mathrm{Ma}_z^2} + \frac{\gamma-1}{2}\mathrm{Ma}_\theta^2\, du_\theta^2 - dq - d\gamma - dR \\
&= -2\frac{\left(1 + \frac{\gamma-1}{2}\mathrm{Ma}_z^2\right)}{1 - \mathrm{Ma}_z^2}dr^2 - \frac{\left(1 + \frac{\gamma-1}{2}\mathrm{Ma}_z^2\right)}{1 - \mathrm{Ma}_z^2}(\gamma-1)\mathrm{Ma}_\theta^2\, du_\theta^2 + \frac{\gamma-1}{2}\mathrm{Ma}_\theta^2\, du_\theta^2 + \frac{1 + \gamma\mathrm{Ma}_z^2}{1 - \mathrm{Ma}_z^2}dq + \frac{1 + \gamma\mathrm{Ma}_z^2}{1 - \mathrm{Ma}_z^2}dR - d\gamma \\
&\quad but \quad du_\theta^2 = -dr^2 \quad from\ (30), \quad \Rightarrow \\
&= -2\frac{\left(1 + \frac{\gamma-1}{2}\mathrm{Ma}_z^2\right)}{1 - \mathrm{Ma}_z^2}dr^2 + \frac{\left(1 + \frac{\gamma-1}{2}\mathrm{Ma}_z^2\right)}{1 - \mathrm{Ma}_z^2}(\gamma-1)\mathrm{Ma}_\theta^2\, dr^2 - \frac{\gamma-1}{2}\mathrm{Ma}_\theta^2\, dr^2 + \frac{1 + \gamma\mathrm{Ma}_z^2}{1 - \mathrm{Ma}_z^2}dq + \frac{1 + \gamma\mathrm{Ma}_z^2}{1 - \mathrm{Ma}_z^2}dR - d\gamma \\
&= -\left[2\frac{\left(1 + \frac{\gamma-1}{2}\mathrm{Ma}_z^2\right)}{1 - \mathrm{Ma}_z^2}\left(1 - \frac{\gamma-1}{2}\mathrm{Ma}_\theta^2\right) + \frac{\gamma-1}{2}\mathrm{Ma}_\theta^2\right]dr^2 + \frac{1 + \gamma\mathrm{Ma}_z^2}{1 - \mathrm{Ma}_z^2}dq + \frac{1 + \gamma\mathrm{Ma}_z^2}{1 - \mathrm{Ma}_z^2}dR - d\gamma
\end{aligned}
\tag{59}
$$

If S is defined as:

$$
S(\gamma, \mathrm{Ma}_\theta) \doteq \frac{\gamma-1}{2}\mathrm{Ma}_\theta^2 \tag{60}
$$

DOI: 10.13009/EUCASS2025-437

thus Eq. (59) can be rearranged as follow:

$$\begin{aligned} d\mathrm{Ma}_z^2 &= -\left[2\frac{\left(1+\frac{\gamma-1}{2}\mathrm{Ma}_z^2\right)}{1-\mathrm{Ma}_z^2}(1-S)+S\right]dr^2+\frac{1+\gamma\mathrm{Ma}_z^2}{1-\mathrm{Ma}_z^2}dq+\frac{1+\gamma\mathrm{Ma}_z^2}{1-\mathrm{Ma}_z^2}dR-d\gamma \\ &= -\left[2\frac{\left(1+\frac{\gamma-1}{2}\mathrm{Ma}_z^2\right)}{1-\mathrm{Ma}_z^2}-2\frac{\left(1+\frac{\gamma-1}{2}\mathrm{Ma}_z^2\right)}{1-\mathrm{Ma}_z^2}S+S\right]dr^2+\frac{1+\gamma\mathrm{Ma}_z^2}{1-\mathrm{Ma}_z^2}dq+\frac{1+\gamma\mathrm{Ma}_z^2}{1-\mathrm{Ma}_z^2}dR-d\gamma \\ &= -\left[2\frac{\left(1+\frac{\gamma-1}{2}\mathrm{Ma}_z^2\right)}{1-\mathrm{Ma}_z^2}+\frac{-2-\gamma\mathrm{Ma}_z^2+\cancel{\mathrm{Ma}_z^2}+1-\cancel{\mathrm{Ma}_z^2}}{1-\mathrm{Ma}_z^2}S\right]dr^2+\frac{1+\gamma\mathrm{Ma}_z^2}{1-\mathrm{Ma}_z^2}dq+\frac{1+\gamma\mathrm{Ma}_z^2}{1-\mathrm{Ma}_z^2}dR-d\gamma \\ &= -\left[2\frac{\left(1+\frac{\gamma-1}{2}\mathrm{Ma}_z^2\right)}{1-\mathrm{Ma}_z^2}-\frac{1+\gamma\mathrm{Ma}_z^2}{1-\mathrm{Ma}_z^2}S\right]dr^2+\frac{1+\gamma\mathrm{Ma}_z^2}{1-\mathrm{Ma}_z^2}dq+\frac{1+\gamma\mathrm{Ma}_z^2}{1-\mathrm{Ma}_z^2}dR-d\gamma \end{aligned} \tag{61}$$

Therefore:

$$d\mathrm{Ma}_z^2=\left(-2\frac{1+\frac{\gamma-1}{2}\mathrm{Ma}_z^2}{1-\mathrm{Ma}_z^2}+\frac{1+\gamma\mathrm{Ma}_z^2}{1-\mathrm{Ma}_z^2}S\right)dr^2+\left(\frac{1+\gamma\mathrm{Ma}_z^2}{1-\mathrm{Ma}_z^2}\right)dq+\left(\frac{1+\gamma\mathrm{Ma}_z^2}{1-\mathrm{Ma}_z^2}\right)dR+(-1)\,d\gamma \tag{62}$$

Matrix row 3

Starting from Eq. (58) final result:

$$du_z=-\frac{1}{1-\mathrm{Ma}_z^2}dr^2+\frac{1}{1-\mathrm{Ma}_z^2}S\,dr^2+\frac{1}{1-\mathrm{Ma}_z^2}dq+\frac{1}{1-\mathrm{Ma}_z^2}dR$$

thus

$$du_z=\left(-\frac{1}{1-\mathrm{Ma}_z^2}+\frac{1}{1-\mathrm{Ma}_z^2}S\right)dr^2+\left(\frac{1}{1-\mathrm{Ma}_z^2}\right)dq+\left(\frac{1}{1-\mathrm{Ma}_z^2}\right)dR+(0)\,d\gamma \tag{63}$$

Matrix row 4

Result is implicit in Eq. (30):

$$du_\theta=\left(-\frac{1}{2}\right)dr^2+(0)dq+(0)dR+(0)d\gamma \tag{64}$$

Matrix row 5

From Eq. (10):

$$da=du-\frac{1}{2}d\mathrm{Ma}_z^2$$

but from Eq. (62) *and* (63)

$$\begin{aligned} &=\left(\cancel{-\frac{1}{1-\mathrm{Ma}_z^2}}+\frac{1}{1-\mathrm{Ma}_z^2}S+\frac{\cancel{1}+\frac{\gamma-1}{2}\mathrm{Ma}_z^2}{1-\mathrm{Ma}_z^2}-\frac{1}{2}\frac{1+\gamma\mathrm{Ma}_z^2}{1-\mathrm{Ma}_z^2}S\right)dr^2+ \\ &\quad+\left(\frac{1}{1-\mathrm{Ma}_z^2}-\frac{1}{2}\frac{1+\gamma\mathrm{Ma}_z^2}{1-\mathrm{Ma}_z^2}\right)dq+\left(\frac{1}{1-\mathrm{Ma}_z^2}-\frac{1}{2}\frac{1+\gamma\mathrm{Ma}_z^2}{1-\mathrm{Ma}_z^2}\right)dR+\left(\frac{1}{2}\right)d\gamma \\ &=\left(\frac{(\gamma-1)\mathrm{Ma}_z^2}{2(1-\mathrm{Ma}_z^2)}+\frac{2-1-\gamma\mathrm{Ma}_z^2}{2(1-\mathrm{Ma}_z^2)}S\right)dr^2+\left(\frac{2-1-\gamma\mathrm{Ma}_z^2}{2(1-\mathrm{Ma}_z^2)}\right)dq+\left(\frac{2-1-\gamma\mathrm{Ma}_z^2}{2(1-\mathrm{Ma}_z^2)}\right)dR+\left(\frac{1}{2}\right)d\gamma \end{aligned}$$

thus

$$da=\left(\frac{(\gamma-1)\,\mathrm{Ma}_z^2}{2\left(1-\mathrm{Ma}_z^2\right)}+\frac{1-\gamma\mathrm{Ma}_z^2}{2(1-\mathrm{Ma}_z^2)}S\right)dr^2+\left(\frac{1-\gamma\mathrm{Ma}_z^2}{2\left(1-\mathrm{Ma}_z^2\right)}\right)dq+\left(\frac{1-\gamma\mathrm{Ma}_z^2}{2\left(1-\mathrm{Ma}_z^2\right)}\right)dR+\left(\frac{1}{2}\right)d\gamma \tag{65}$$

DOI: 10.13009/EUCASS2025-437

Matrix row 2

From Eq. (10):

$$d\mathrm{Ma}_\theta^2 = 2(du_\theta - da)$$

but from Eq. (65) *and* (64)

$$= 2\left(-\frac{1}{2} - \frac{(\gamma-1)\,\mathrm{Ma}_z^2}{2\left(1-\mathrm{Ma}_z^2\right)} - \frac{1-\gamma\mathrm{Ma}_z^2}{2(1-\mathrm{Ma}_z^2)}S\right)dr^2 - 2\left(\frac{1-\gamma\mathrm{Ma}_z^2}{2\left(1-\mathrm{Ma}_z^2\right)}\right)dq - 2\left(\frac{1-\gamma\mathrm{Ma}_z^2}{2\left(1-\mathrm{Ma}_z^2\right)}\right)dR - 2\left(\frac{1}{2}\right)d\gamma$$
$$= \left(-\frac{1-\mathrm{Ma}_z^2+(\gamma-1)\mathrm{Ma}_z^2}{1-\mathrm{Ma}_z^2} - \frac{1-\gamma\mathrm{Ma}_z^2}{1-\mathrm{Ma}_z^2}S\right)dr^2 + \left(-\frac{1-\gamma\mathrm{Ma}_z^2}{1-\mathrm{Ma}_z^2}\right)dq + \left(-\frac{1-\gamma\mathrm{Ma}_z^2}{1-\mathrm{Ma}_z^2}\right)dR + (-1)d\gamma$$

thus

$$d\mathrm{Ma}_\theta = \left(-\frac{1+(\gamma-2)\mathrm{Ma}_z^2}{1-\mathrm{Ma}_z^2} - \frac{1-\gamma\mathrm{Ma}_z^2}{1-\mathrm{Ma}_z^2}S\right)dr^2 + \left(-\frac{1-\gamma\mathrm{Ma}_z^2}{1-\mathrm{Ma}_z^2}\right)dq + \left(-\frac{1-\gamma\mathrm{Ma}_z^2}{1-\mathrm{Ma}_z^2}\right)dR + (-1)d\gamma \tag{66}$$

Matrix row 6

From Eq. (7)

$$dT = 2da - d\gamma - dR$$

but from Eq. (65)

$$= 2\left(\frac{(\gamma-1)\,\mathrm{Ma}_z^2}{2\left(1-\mathrm{Ma}_z^2\right)} + \frac{1-\gamma\mathrm{Ma}_z^2}{2(1-\mathrm{Ma}_z^2)}S\right)dr^2 + \left(2\frac{1-\gamma\mathrm{Ma}_z^2}{2\left(1-\mathrm{Ma}_z^2\right)}\right)dq + \left(2\frac{1-\gamma\mathrm{Ma}_z^2}{2\left(1-\mathrm{Ma}_z^2\right)} - 1\right)dR + \left(2\frac{1}{2} - 1\right)d\gamma$$
$$= \left(\frac{(\gamma-1)\,Ma_z^2}{1-\mathrm{Ma}_z^2} + \frac{1-\gamma\mathrm{Ma}_z^2}{1-\mathrm{Ma}_z^2}S\right)dr^2 + \left(\frac{1-\gamma\mathrm{Ma}_z^2}{1-\mathrm{Ma}_z^2}\right)dq + \left(\frac{1-\gamma\mathrm{Ma}_z^2-1+\mathrm{Ma}_z^2}{1-\mathrm{Ma}_z^2}\right)dR + (0)d\gamma$$

thus

$$dT = \left(\frac{(\gamma-1)\,Ma_z^2}{1-\mathrm{Ma}_z^2} + \frac{1-\gamma\mathrm{Ma}_z^2}{1-\mathrm{Ma}_z^2}S\right)dr^2 + \left(\frac{1-\gamma\mathrm{Ma}_z^2}{1-\mathrm{Ma}_z^2}\right)dq + \left(\frac{(1-\gamma)\,\mathrm{Ma}_z^2}{1-\mathrm{Ma}_z^2}\right)dR + (0)d\gamma \tag{67}$$

Matrix row 7

From Eq. (17):

$$d\rho = -du_z - dr^2$$

but from Eq. (63)

$$= \left(\frac{1}{1-\mathrm{Ma}_z^2} - \frac{1}{1-\mathrm{Ma}_z^2}S - 1\right)dr^2 - \left(\frac{1}{1-\mathrm{Ma}_z^2}\right)dq - \left(\frac{1}{1-\mathrm{Ma}_z^2}\right)dR + (0)\,d\gamma$$

thus

$$d\rho = \left(\frac{\mathrm{Ma}_z^2}{1-\mathrm{Ma}_z^2} - \frac{1}{1-\mathrm{Ma}_z^2}S\right)dr^2 + \left(-\frac{1}{1-\mathrm{Ma}_z^2}\right)dq + \left(-\frac{1}{1-\mathrm{Ma}_z^2}\right)dR + (0)d\gamma \tag{68}$$

DOI: 10.13009/EUCASS2025-437

Matrix row 8

From Eq. (5):

$$dp = d\rho + dT + dR$$

but from Eq. (67) *and* (68)

$$\begin{aligned}
&= \left(\frac{\mathrm{Ma}_z^2}{1-\mathrm{Ma}_z^2} - \frac{1}{1-\mathrm{Ma}_z^2}S + \frac{(\gamma-1)\,Ma_z^2}{1-\mathrm{Ma}_z^2} + \frac{1-\gamma\mathrm{Ma}_z^2}{1-\mathrm{Ma}_z^2}S\right)dr^2 + \\
&+ \left(-\frac{1}{1-Ma_z^2} + \frac{1-\gamma\mathrm{Ma}_z^2}{1-\mathrm{Ma}_z^2}\right)dq + \left(-\frac{1}{1-\mathrm{Ma}_z^2} + \frac{(1-\gamma)\,\mathrm{Ma}_z^2}{1-\mathrm{Ma}_z^2} + 1\right)dR \\
&= \left(\frac{\gamma\mathrm{Ma}_z^2}{1-\mathrm{Ma}_z^2} - \frac{\gamma\mathrm{Ma}_z^2}{1-\mathrm{Ma}_z^2}S\right)dr^2 + \left(-\frac{\gamma\mathrm{Ma}_z^2}{1-\mathrm{Ma}_z^2}\right)dq + \left(\frac{-1+\mathrm{Ma}_z^2 - \gamma\mathrm{Ma}_z^2 + 1-\mathrm{Ma}_z^2}{1-\mathrm{Ma}_z^2}\right)dR
\end{aligned}$$

thus

$$dp = \left(\frac{\gamma\mathrm{Ma}_z^2}{1-\mathrm{Ma}_z^2} - \frac{\gamma\mathrm{Ma}_z^2}{1-\mathrm{Ma}_z^2}S\right)dr^2 + \left(-\frac{\gamma\mathrm{Ma}_z^2}{1-\mathrm{Ma}_z^2}\right)dq + \left(-\frac{\gamma\mathrm{Ma}_z^2}{1-\mathrm{Ma}_z^2}\right)dR + (0)d\gamma \tag{69}$$

Matrix row 9

From Eq. (14)

$$ds = dT - \frac{\gamma-1}{\gamma}dp$$

but from Eq. (67) *and* (69)

$$\begin{aligned}
&= \left(\frac{(\gamma-1)\,Ma_z^2}{1-\mathrm{Ma}_z^2} + \frac{1-\gamma\mathrm{Ma}_z^2}{1-\mathrm{Ma}_z^2}S\right)dr^2 + \left(\frac{1-\gamma\mathrm{Ma}_z^2}{1-\mathrm{Ma}_z^2}\right)dq + \left(\frac{(1-\gamma)\,\mathrm{Ma}_z^2}{1-\mathrm{Ma}_z^2}\right)dR + \\
&- \frac{\gamma-1}{\gamma}\left(\frac{\gamma\mathrm{Ma}_z^2}{1-\mathrm{Ma}_z^2} - \frac{\gamma\mathrm{Ma}_z^2}{1-\mathrm{Ma}_z^2}S\right)dr^2 - \frac{\gamma-1}{\gamma}\left(-\frac{\gamma\mathrm{Ma}_z^2}{1-\mathrm{Ma}_z^2}\right)dq - \frac{\gamma-1}{\gamma}\left(-\frac{\gamma\mathrm{Ma}_z^2}{1-\mathrm{Ma}_z^2}\right)dR
\end{aligned} \tag{70}$$

All the terms simplifies except for S and dq. Thus:

$$ds = (S)dr^2 + (1)dq + (0)dR + (0)d\gamma \tag{71}$$